ADVANCED FUNCTIONAL MATERIALS

FULL PAPER

DOI: 10.1002/adfm.200500933

Formation of Metal Nano- and Micropatterns on Self-Assembled Monolayers by Pulsed Laser Deposition Through Nanostencils and Electroless Deposition**

By *Emiel A. Speets*, *Paul te Riele*, *Marc A. F. van den Boogaart*, *Lianne M. Doeswijk*, *Bart Jan Ravoo*,* *Guus Rijnders*, *Jürgen Brugger*,* *David N. Reinhoudt*,* and *Dave H. A. Blank**

Patterns of noble-metal structures on top of self-assembled monolayers (SAMs) on Au and SiO_2 substrates have been prepared following two approaches. The first approach consists of pulsed laser deposition (PLD) of Pt, Pd, Au, or Cu through nano- and microstencils. In the second approach, noble-metal cluster patterns deposited through nano- and microstencils are used as catalysts for selective electroless deposition (ELD) of Cu. Cu structures are grown on SAMs on both Au and SiO_2 substrates and are subsequently analyzed using X-ray photoelectron spectroscopy element mapping, atomic force microscopy, and optical microscopy. The combination of PLD through stencils on SAMs followed by ELD is a new method for the creation of (sub)-micrometer-sized metal structures on top of SAMs. This method minimizes the gas-phase deposition step, which is often responsible for damage to, or electrical shorts through, the SAM.

1. Introduction

Permanent (sub)-micrometer-sized electrodes on self-assembled monolayers (SAMs) are important in molecular electronic devices[1] but are challenging to fabricate.[2] The deposition of a top electrode might damage the SAM, and diffusion of the deposited metal might cause shorts between the electrodes. The creation of stable metal contacts on top of SAMs on Au is difficult because of the liquid-crystalline character and the characteristic thickness (ca. 2 nm) of the SAM. Deposited metal can diffuse through the SAM and form adlayers at the sulfur/gold interface. Destruction of the SAM by the incoming atoms with high kinetic energy is another risk, which can be only partially countered by cooling the sample.[3]

Recently Rogers and co-workers[4–6] developed so-called metal nanotransfer printing, in which a polydimethylsiloxane (PDMS) stamp is used to transfer a thin film of Au from the stamp onto a thiol-terminated SAM on gallium arsenide or silicon dioxide. The thiol-terminated SAM acts as a "glue" for the Au film, ensuring the transfer. The advantage of this technique is that Au is transferred in a continuous (bulk) layer and not as single atoms, like in vapor deposition techniques. To facilitate the transfer process, an antisticking, hydrophobic, perfluoro-terminated SAM was deposited on the oxidized PDMS stamp. On the other hand, a gas-phase technique might be advantageous because such a process is cleaner and PDMS stamps usually leave silicone traces on the sample.

Electroless deposition (ELD) is a method that can be used to create metal patterns on surfaces via solution electrochemistry. ELD on a substrate uses a pre-existing pattern of a catalytic species to form the desired metal pattern.[7] It has been used in combination with several patterning techniques such as microcontact printing,[8] photolithography,[9] and electron-beam (e-beam) lithography.[10] A patterned metal(0) surface can be formed by chemically reducing metal ions bound to a surface and can act as a catalyst for the initiation of ELD.[11,12] Chelated metal ions can subsequently be reduced on a metal(0) surface by a reductor present in solution according to the ELD principle.

Stencils are a convenient "top-down" tool for the deposition of metal structures on surfaces. Nanostencils have been used as shadow masks for the deposition of Au dots with heights of 150 nm on SiO_2 by evaporation.[13,14] Wafer-sized micro- and nanostencils have been fabricated and successfully applied in the direct multiple-length-scale surface patterning of, for example, Al.[15] Previously we have shown that pulsed laser deposition (PLD) can be used in combination with nanostencils as a

[*] Dr. B. J. Ravoo, Prof. D. N. Reinhoudt, Dr. E. A. Speets
Laboratory of Supramolecular Chemistry and Technology
MESA+ Institute for Nanotechnology
P.O. Box 217, 7500 AE, Enschede (The Netherlands)
E-mail: b.j.ravoo@utwente.nl; d.n.reinhoudt@utwente.nl
Prof. D. H. A. Blank, P. te Riele, Dr. G. Rijnders
Inorganic Materials Science Group
MESA+ Institute for Nanotechnology
P.O. Box 217, 7500 AE, Enschede (The Netherlands)
E-mail: d.h.a.blank@utwente.nl
Prof. J. Brugger, M. A. F. van den Boogaart, Dr. L. M. Doeswijk
Microsystems Laboratory 1
Institute of Microelectronics and Microsystems
Ecole Polytechnique Federale Lausanne
1015 Lausanne (Switzerland)
E-mail: juergen.brugger@epfl.ch

[**] We acknowledge the Nanolink program of the MESA+ Institute for Nanotechnology and the European FP6 Integrated project NaPa (contract no. NMP4-CT-2003-500120) for financial support. The content of this work is the sole responsibility of the authors.

useful technique for the deposition of top electrodes on SAMs.[16] In PLD it is possible to deposit metal at elevated pressures, which leads to deposition of thermalized metal particles on the substrate. For deposition of metals on SAMs this has several advantages: the incident metal will not damage the SAM, and clusters formed in the plasma at higher pressures are less likely to diffuse through pinholes in the SAM. We have demonstrated the deposition of Au islands (ca. 700 nm in diameter) on octadecanethiol (ODT) SAMs. 15 % of the islands were insulated from the bottom electrode by the ca. 2 nm thick SAM.[16,17] PLD was also used to deposit insulated nanometer-sized noble-metal clusters on SAMs.[18,19] These insulated metal clusters are stable on methyl-terminated SAMs and show Coulomb blockade at room temperature.

We felt that a general method is needed for the deposition of metal structures on SAMs with dimensions ranging from the nano- to the microscale. In this article, we describe two methods. First, we directly deposit metals by PLD through nano- and microstencils yielding structures with sizes ranging from 500 nm to a few hundred micrometers. Second, we deposit minimal amounts of metal on SAMs, and use these as a catalyst for ELD of Cu (Fig. 1). The noble-metal clusters described in a previous publication[18] were deposited through stencils to create catalytic templates on the SAMs. In previous studies, we used SAMs of thiolates on Au substrates; in this paper, we also describe the deposition on SAMs of octadecyltrichlorosilane (ODTS) on SiO_2.

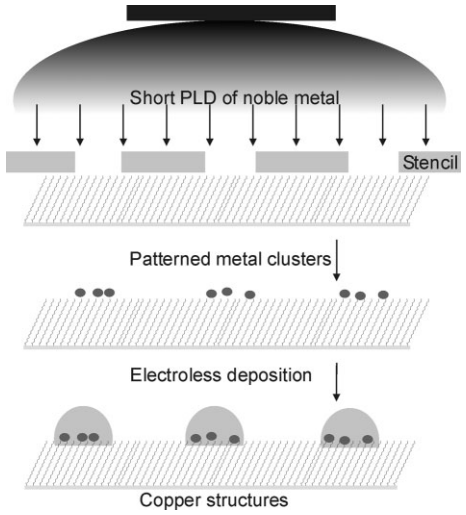

Figure 1. Schematic representation of metal pattern-enhancement on SAMs by ELD of copper after PLD of a noble metal through a stencil.

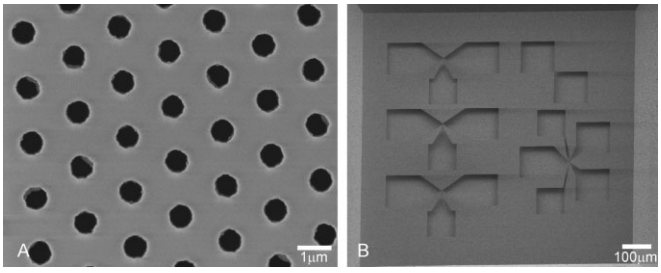

Figure 2. Scanning electron microscopy (SEM) image of A) a Si_3N_4 nanostencil with 500 nm diameter pores and B) part of a microstencil.

2. Results and Discussion

2.1. Microstencils and Nanostencils

In this study, Si_3N_4 membranes supported by a silicon chip have been used as stencils for the patterned deposition of metals on SAMs. The nanostencils have holes with a diameter of approximately 500 nm, that are arranged in a hexagonal pattern with a center-to-center spacing of 1.6 μm. We also used microstencils that contain features with sizes ranging from 500 nm to hundreds of micrometers in the same membrane. The size of the stencils is 2.5 cm × 2.5 cm and they contain 25 freestanding 1 mm × 1 mm Si_3N_4 membranes with a thickness of 200 nm, each with a different pattern.[20] In Figures 2A and B images of a nanostencil and microstencil are shown.

2.2. PLD of Metal Structures on SAMs

Atomic force microscopy (AFM) has been used to image the deposited structures. The AFM scans show the deposition of Pd (Fig. 3), Cu (Fig. 4), and Pt (Fig. 5) through nanostencils on ODT SAMs on Au. The hexagonal array of the holes in the nanostencil is faithfully replicated as a hexagonal pattern of metal islands. The islands are approximately 500–700 nm in diameter and 3–4 nm in height. The broadening of the deposited islands relative to the diameter of the holes in the stencil is caused mainly by the gap between the stencil and the substrate. Especially when depositing at higher pressures (≳0.001 mbar (≳0.1 Pa)) the metal plasma is more diffuse, which leads to enlargement of the area on which deposition takes place. Local distortion of the stencil or misalignment of the substrate with the central axis of the plasma can lead to variation in shape of the deposited features.

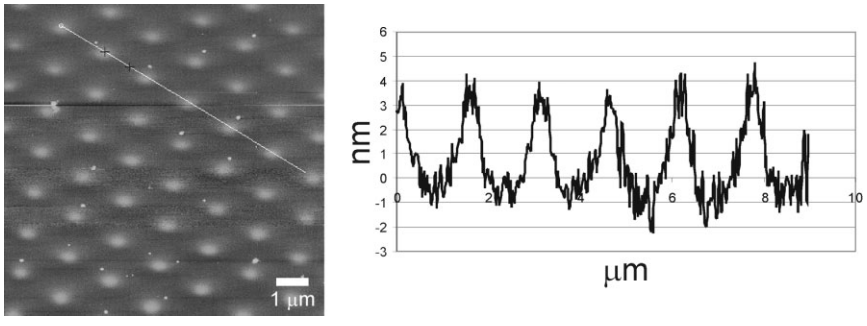

Figure 3. AFM height image and section analysis of Pd islands made by PLD through a nanostencil on an ODT SAM (pressure, $p = 0.001$ mbar (0.1 Pa); distance between target and substrate, $d = 40$ mm, scan time, $t = 4$ min at 8 Hz (1920 pulses), spot size ca. 1.76 mm^2, fluence 4 J cm^{-2}).

ADVANCED FUNCTIONAL MATERIALS

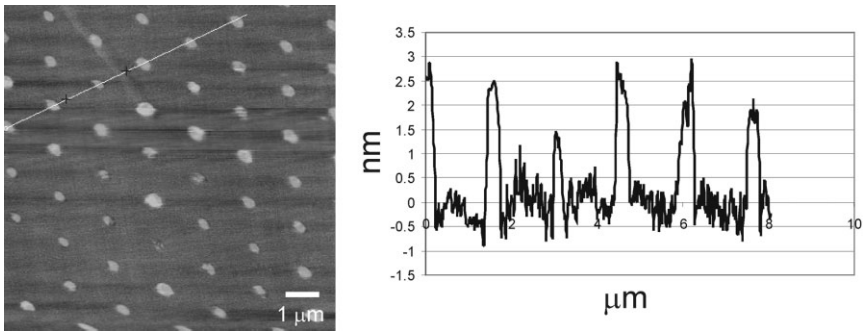

Figure 4. AFM height image and section analysis of Cu islands made by PLD through a nanostencil on an ODT SAM ($p = 0.001$ mbar, $d = 40$ mm, $t = 4$ min at 8 Hz (1920 pulses), spot size ca. 2.97 mm^2, fluence 3.5 J cm^{-2}).

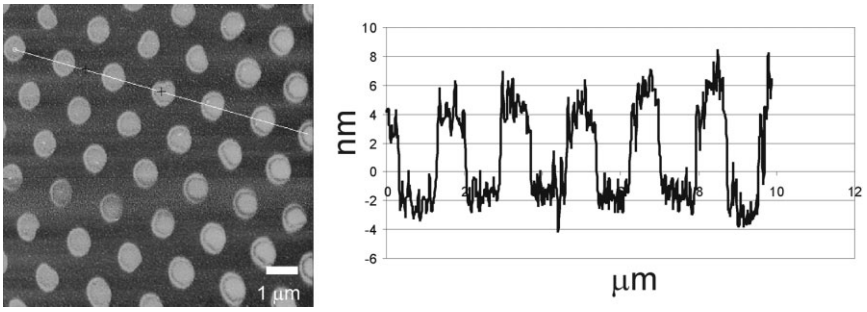

Figure 5. AFM height image and section analysis of Pt islands made by PLD through a nanostencil on an ODT SAM ($p = 0.001$ mbar, $d = 40$ mm, $t = 2$ min at 8 Hz (960 pulses), fluence 5.0 J cm^{-2}).

These observations are consistent with previously published results for the deposition of Au on ODT SAMs.[16] In these previous experiments, X-ray photoelectron spectroscopy (XPS) and friction AFM measurements showed that the metal islands expose bare metal surfaces that are not covered by the SAM.[16] However, we cannot exclude limited diffusion of the noble metals through the unreactive ODT SAM.[21] The amount of deposited material could be controlled by the number of pulses used to ablate the target. The background pressure, the distance between the target and substrate, and the laser fluence can be varied to further control the deposition.

Pt and Pd were also deposited on ODT SAMs on Au via PLD through microstencils, yielding larger metal structures. Pt and Pd deposited through a microstencil on SAMs on Au can be visualized using XPS element mapping. Using a scanning X-ray beam with a spot diameter of ca. 9 μm, an area of up to 1 mm × 1 mm can be scanned for the element of choice. In the XPS element maps the patterns present in the microstencil are clearly visible (Fig. 6). XPS imaging is especially valuable if small amounts of metal are deposited that are difficult to detect using, for example, AFM or optical microscopy. Deposited features consisting of metal particles that do not cover the whole surface are difficult to detect with AFM, because of the lack of height and friction contrast with the substrate. Optical microscopy is also not an option if only small amounts of material are deposited, since the optical contrast is not sufficient.

2.3. ELD on Metal Patterns Deposited on SAMs

In the second approach, noble metals were deposited by PLD through nano- and microstencils and the metal pattern was enhanced in Cu by immersion in an ELD plating bath (see Fig. 1). After only 60 laser pulses of Pt on an ODTS SAM on SiO_2 through a microstencil (holes with micrometer dimensions), no Pt pattern was detected by AFM. However, we have previously demonstrated that these PLD conditions lead to the deposition of Pt nanoclusters.[18] Immersion of the sample for 15 s in an ELD solution develops the pattern deposited in Pt as 30 nm high Cu structures (Fig. 7). The structures measuring around 5 μm × 8 μm can be detected easily with AFM. As can be seen in Figure 7, no Cu growth took place in between the pulsed-laser-deposited structures, indicating that the deposited Pt does not diffuse on the hydrophobic SAM of the sample during or after PLD. The pattern of Pt clusters is a template for the formation of Cu microstructures.

More challenging is ELD on metal-cluster patterns deposited on SAMs on Au. Any damage caused by the deposition process or disorder in the SAM would lead to uncontrolled ELD because pinholes to the Au substrate will also catalyze ELD. Another problem is the potential diffusion of deposited metal through the SAM,[22] making the deposited material unavailable for use as an ELD catalyst. Pt was also used as Cu-ELD catalyst on ODT SAMs on Au. In Figure 8, AFM height scans of a sample containing Pt islands before and after Cu ELD are shown. After 240 pulses Pt islands with a height of 2 nm are present, as can be seen in the AFM image (Fig. 8A). The sample was immersed in an ELD solution for one minute, which resulted in the deposition of ca. 60 nm of Cu on the Pt template.

Optical microscopy can be used to visualize metal patterns on the SAM substrates when the metals are deposited using

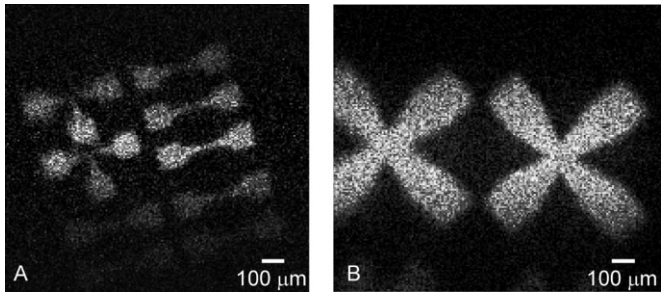

Figure 6. XPS element maps of A) Pd of Pd deposited on an ODT SAM on Au, and B) Pt of Pt deposited on an ODT SAM on Au (signal increases from dark to light).

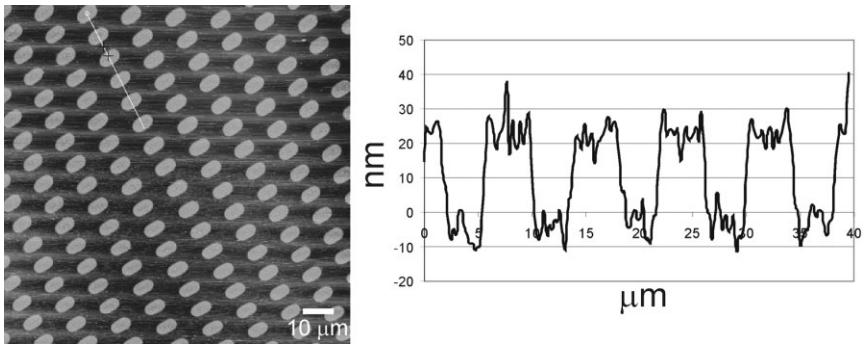

Figure 7. AFM height image of ODTS SAM on SiO_2 with deposited Pt structures after 15 s ELD of Cu (PLD at $p = 0.01$ mbar, $t = 15$ s at 4 Hz (60 pulses), fluence 5.0 J cm^{-2}, $d = 40$ mm; see Experimental section for ELD conditions).

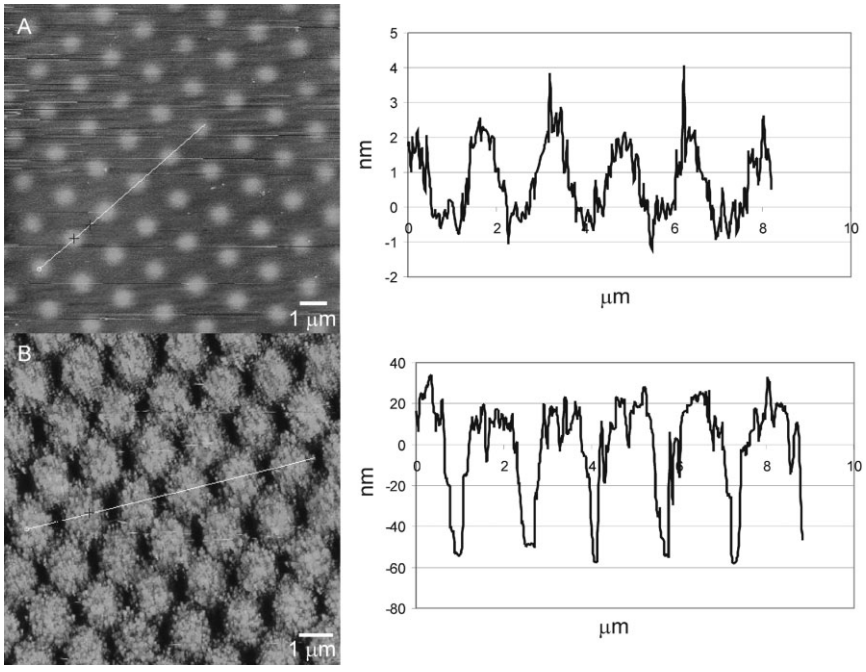

Figure 8. AFM height images and section analyses of A) an ODT SAM on Au with 240 pulses of Pt ($d = 40$ mm, $p = 0.001$ mbar, fluence 5 J cm^{-2}) and B) the same sample after 1 min ELD of Cu. Scan size: 10 μm × 10 μm.

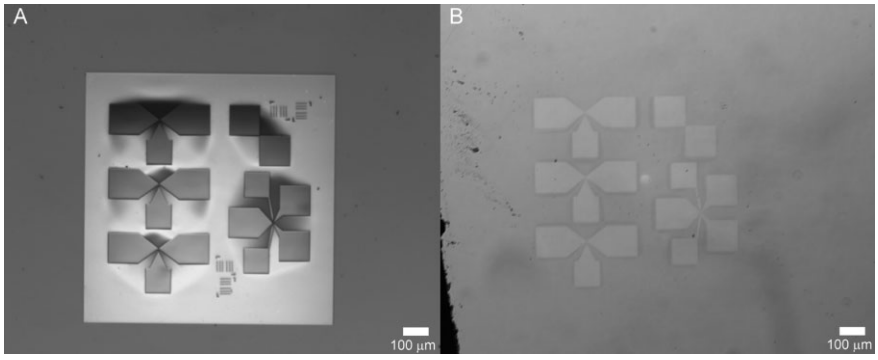

Figure 9. Optical microscopy images of A) details of the microstencil and B) the ODT SAM after 120 pulses of Au have been deposited through the corresponding part of the microstencil via PLD ($p = 0.01$ mbar, $d = 40$ mm, fluence 4 J cm^{-2}) and 2 min ELD of Cu.

PLD through microstencils and the patterns are enhanced by ELD. No height information can be obtained, but the extent of ELD and possible overgrowth can be easily detected. In Figure 9 it can be seen that the patterns in the Si_3N_4 stencil (Fig. 9A) have been faithfully reproduced on the ODT SAM by PLD of Au followed by Cu ELD. ELD deposition on these structures shows that the SAM around the structures protects the Au substrate from ELD, while the (uncovered) Au pattern catalyzes the deposition of Cu. In addition, Pd was deposited by PLD on an ODTS SAM on SiO_2, after which the pattern was enhanced using ELD. In the example shown in Figure 10 we used only 40 pulses of Pd, after which the sample was immersed for five minutes in an ELD solution. The structure in the right upper corner (Fig. 10B) is only partly enhanced with Cu, suggesting that in this particular experiment the amount of Pd that was deposited by PLD is close to the lower limit of catalyst required.

Larger structures deposited through microstencils[19] can be accurately analyzed with XPS element mapping. In Figure 11 three element maps are shown that were obtained after PLD of Pt (Fig. 11, Pt and Au) and after subsequent Cu ELD (Fig. 11, Cu). As can be seen, the pattern that was first deposited by PLD of Pt is now enhanced as a Cu pattern. No Pt could be detected after ELD, indicating that Pt is totally covered by Cu during ELD. The Au map shows the negative image of the Pt and Cu maps. No Au could be detected in the area where first Pt and then Cu was deposited. This indicates that the thickness of the SAM plus the deposited Pt is at least > 5 nm, which is the penetration depth of XPS at these conditions (see Experimental section).

3. Conclusion

PLD was successfully used in combination with micro- and nanostencils to deposit patterns of Pt, Pd, Cu, and Au on SAMs. Metal nanostructures were prepared on ODT SAMs on Au and on ODTS SAMs on SiO_2. AFM, optical microscopy, and XPS element mapping were used to visualize the structures with sizes ranging from 500 nm to several hundred

ADVANCED FUNCTIONAL MATERIALS

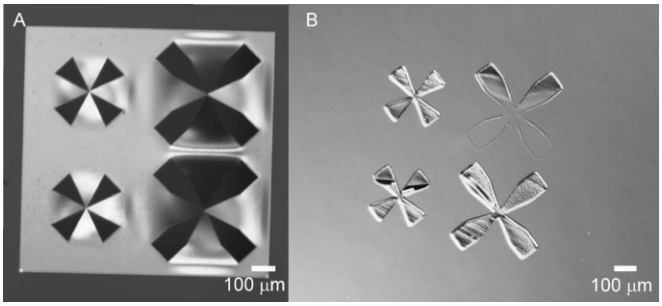

Figure 10. Optical microscopy images of A) details of the microstencil and B) ODTS SAM after 40 pulses of Pd have been deposited through the corresponding part of the microstencil via PLD ($p = 0.01$ mbar, $d = 40$ mm, fluence 4 J cm^{-2}) and 5 min ELD of Cu.

micrometers. In an alternative approach, the structures of metal deposited on SAMs by PLD were used to catalyze electroless ELD of Cu, creating features of Cu on the SAMs. The combination of a short gas-phase deposition followed by ELD from solution is useful if substrates are not stable under prolonged gas-phase deposition. The SAMs protect the underlying Au substrate from the ELD solution, so that Cu growth takes place only on the patterns defined by the stencil. The methods presented here will be useful in increasing the yield of metal–SAM–metal junctions without short circuits.

4. Experimental

4.1. SAMs

Octadecanethiol SAMs were prepared from ca. 1 mM solutions of octadecanethiol (98 %, Janssen Chimica) in ethanol (pa, Merck). Gold substrates (20 nm gold on 2 nm Ti on Si (p <001>)) were obtained from Ssens (Hengelo, The Netherlands). Substrates were rinsed with dichloromethane (pa, Biosolve) before use and immersed in the ethanol solutions for at least 12 h. After removing from solution, the substrates were rinsed with dichloromethane pa, ethanol pa, and water (MilliQ). SAMs on SiO_2 were prepared from a 0.1 vol % solution of octadecyltrichlorosilane (95 %, Acros) in toluene. Silicon chips (p-type <001>) were immersed in fresh piranha solution (three parts H_2SO_4, one part H_2O_2 for 15 min (CAUTION: piranha solution should not come in contact with organic material). The substrates were rinsed with large amounts of water and dried in a nitrogen stream. The Si chips were immersed in the ODTS solutions for 2 h in a glove box. The substrates were removed and rinsed with toluene in the glove box. The substrates were further rinsed outside the glove box using toluene and dichloromethane. SAMs were analyzed with XPS, contact-angle goniometry, and electrochemistry.

4.2. Pulsed Laser Deposition

PLD was performed using a Compex 205 KrF excimer laser from Lambda Physik with a wavelength of 248 nm, with pulse lengths of 30 ns. The laser was focused through a rectangular mask (102 mm^2) and a lens, and spot sizes on the target were typically around 2.5 mm^2. The laser fluence was approximately 4 J cm^{-2} for Au and Pd, and around 5 J cm^{-2} for Pt. Background pressures ranged from 10^{-3} to 1 mbar.

4.3. X-ray Photoelectron Spectroscopy

XPS was performed on a Physical Electronics Quantera equipped with a monochromatic Al Kα X-ray source (1486.6 eV). Element maps were recorded using an X-ray beam with a diameter of ca. 9 μm (10 pixels per beam width) at ca. 1 W X-ray power. The beam was scanned over an area of typically 1 mm × 1 mm for 30–60 min using a pass energy of 224 eV.

4.3. Electroless Deposition of Copper

Cu ELD was performed using a solution containing 40 mM $CuSO_4$, 140 mM Na_2SO_4, 120 mM Na_4EDTA, 300 mM HC(O)ONa, and 30 mM formaldehyde. After the compounds were dissolved, the pH of the solution was adjusted to 12–13 by the addition of NaOH. A patterned sample (SAM on SiO_2 or Au) was covered with a few drops of this solution for a short period of time (ranging from ten seconds to several minutes depending on the pH of the solution). The samples were then rinsed with water and blown dry in a nitrogen stream.

Received: December 22, 2005
Final version: February 28, 2006
Published online: May 10, 2006

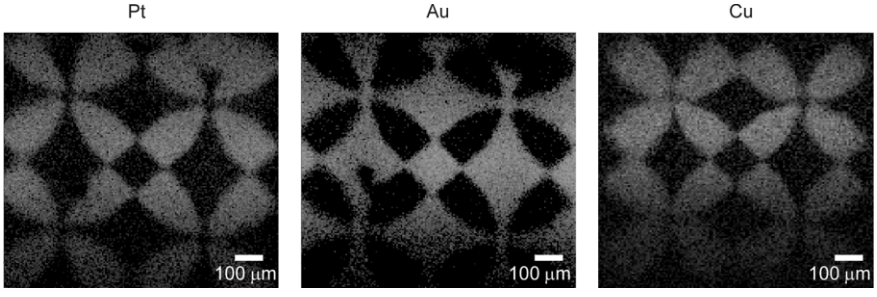

Figure 11. Pt, Au, and Cu XPS element maps of an ODT SAM on Au after Pt deposition through a microstencil (120 pulses of Pt ($d = 40$ mm, $p = 0.01$ mbar, fluence 5 J cm^{-2}) (Pt and Au) and after ELD of Cu (Cu). Dark = low signal; bright = high signal.

[1] a) R. L. Creery, *Chem. Mater.* **2004**, *16*, 4477. b) J.-O. Lee, G. Lientschnig, F. Wiertz, M. Struijk, R. A. J. Janssen, R. Egberink, D. N. Reinhoudt, P. Hadley, C. Dekker, *Nano Lett.* **2003**, *3*, 113.
[2] J. M. Tour, *Molecular Electronics*, World Scientific, Singapore **2003**.
[3] a) J. Chen, M. A. Reed, A. M. Rawlett, J. M. Tour, *Science* **1999**, *286*, 1550. b) T. Lee, W. Wang, J. F. Klemic, J. J. Zhang, J. Su, M. A. Reed, *J. Phys. Chem. B* **2004**, *108*, 8742. c) W. Wang, T. Lee, I. Kretzschmar, M. A. Reed, *Nano Lett.* **2004**, *4*, 643. d) C. Zhou, M. R. Deshpande, M. A. Reed, L. Jones, II, J. M. Tour, *Appl. Phys. Lett.* **1997**, *71*, 611.
[4] Y.-L. Loo, R. L. Willet, K. W. Baldwin, J. A. Rogers, *J. Am. Chem. Soc.* **2002**, *124*, 7654.
[5] Y.-L. Loo, D. V. Lang, J. A. Rogers, J. W. P. Hsu, *Nano Lett.* **2003**, *3*, 913.
[6] E. Menard, L. Bilhaut, J. Zaumseil, J. A. Rogers, *Langmuir* **2004**, *20*, 6871.
[7] a) C. S. Dulsey, J. H. Georger, Jr., V. Krauthammer, D. A. Stenger, T. L. Fare, J. M. Calvert, *Science* **1991**, *252*, 551. b) C. D. Zangmeister, R. D. van Zee, *Langmuir* **2003**, *19*, 8065.

[8] T. B. Carmichael, S. J. Vella, A. Afzali, *Langmuir* **2004**, *20*, 5593.
[9] L. A. Porter, Jr., H. C. Choi, J. M. Schmeltzer, A. E. Ribbe, L. C. C Elliot, J. M. Buriak, *Nano Lett.* **2002**, *2*, 1369.
[10] D. W. Carr, M. J. Lercel, C. S. Whelan, H. G. Craighead, K. Seshadri, D. L. Allara, *J. Vac. Sci. Technol. A* **1997**, *15*, 1446.
[11] H. Kind, A. M. Bittner, O. Cavalleri, K. Kern, T. Greber, *J. Phys. Chem. B* **1998**, *102*, 7582.
[12] P. C. Hidber, W. Helbig, E. Kim, G. M. Whitesides, *Langmuir* **1996**, *12*, 1375.
[13] M. Kolbel, R. W. Tjerkstra, J. Brugger, C. J. M. Van Rijn, W. Nijdam, J. Huskens, D. N. Reinhoudt, *Nano Lett.* **2002**, *2*, 1339.
[14] M. Kolbel, R. W. Tjerkstra, G. Kim, J. Brugger, C. J. M. Van Rijn, W. Nijdam, J. Huskens, D. N. Reinhoudt, *Adv. Funct. Mater.* **2003**, *13*, 219.
[15] G. M. Kim, M. A. F. Van den Boogaart, J. Brugger, *Microelectron. Eng.* **2003**, *67–68*, 609.
[16] E. A. Speets, B. J. Ravoo, F. J. G. Roesthuis, F. Vroegindeweij, D. H. A. Blank, D. N. Reinhoudt, *Nano Lett.* **2004**, *4*, 841.
[17] F. Vroegindeweij, E. A. Speets, J. A. J. Steen, J. Brugger, D. H. A. Blank, *Appl. Phys. A* **2004**, *79*, 743.
[18] E. A. Speets, B. Dordi, B. J. Ravoo, N. Oncel, A.-S. Hallbäck, H. J. W. Zandvliet, B. Poelsema, G. Rijnders, D. H. A. Blank, D. N. Reinhoudt, *Small* **2005**, *1*, 395.
[19] N. Oncel, A.-S. Hallbäck, H. J. W. Zandvliet, E. A. Speets, B. J. Ravoo, D. N. Reinhoudt, B. Poelsema, *J. Chem. Phys.* **2005**, *123*, 044 703.
[20] M. A. F. van den Boogaart, G. M. Kim, R. Pellens, J.-P. van den Heuvel, J. Brugger, *J. Vac. Sci. Technol. B* **2004**, *22*, 3174.
[21] G. C. Herdt, D. R. Jung, A. W. Czanderna, *Prog. Surf. Sci.* **1995**, *25*, 103.
[22] a) B. De Boer, M. M. Frank, Y. J. Chabal, W. Jiang, E. Garfunkel, Z. Bao, *Langmuir* **2004**, *20*, 1539. b) G. L. Fisher, A. V. Walker, A. E. Hooper, T. B. Tighe, K. B. Bahnck, H. T. Skriba, M. D. Reinard, B. C. Haynie, R. L. Opila, N. Winograd, D. L. Allara, *J. Am. Chem. Soc.* **2002**, *124*, 5528.